Inertial and Frictional Effects on Stratified Hydrostatic Airflow past an Isolated Heat Source

YUH-LANG LIN

Department of Marine, Earth, and Atmospheric Sciences, North Carolina State University, Raleigh, North Carolina

(Manuscript received 11 April 1988, in final form 25 September 1988)

ABSTRACT

Inertial and frictional effects on stratified hydrostatic airflow past an isolated warm region are investigated by linear theories. For an inviscid quasi-geostrophic flow, there exists in the lower layer upward motion upstream and downward motion downstream of the warm region. The vertical velocity field is in phase with the diabatic heating and cooling. As expected, regions of high buoyancy, low pressure and positive vorticity are produced in the vicinity of the warm region. Strong vortex stretching occurs near the center of the warm region, accompanied by two regions of weak vortex compression upstream and downstream. With the inertial effects included, the vertical motion and the vorticity are strengthened. The horizontal wind experiences a much stronger cyclonic circulation near the diabatic source.

For a flow with a larger Rossby number $O(1)$, the advection effect of the basic flow is dominant. U-shaped patterns of disturbance are pronounced, which are associated with the upward propagating inertia-gravity waves. The wind is deflected cyclonically around the region of positive relative vorticity and is advected downstream of the center of the warm region, rather than around the region of the low pressure.

The frictional effects are investigated by the addition of an Ekman friction layer to a quasi-geostrophic flow. There are three significant features of the disturbance: (i) an upstream-downstream asymmetry, (ii) an upstream phase tilt in the lower layer, and (iii) weakening of the positive relative vorticity and low pressure. Items (i) and (ii) are explained by the upward motion and vorticity and the advection of the basic flow on the disturbance induced by the Ekman friction. The weakening of the positive relative vorticity and the low pressure can be explained as the spindown process of the interior flow to the Ekman friction.

1. Introduction

The theoretical problem of a stratified flow over a prescribed diabatic heating has received considerable attention in the last three decades. One of the earliest work is by Malkus and Stern (1953) on a two-dimensional flow over a heat island 10 km in width and normal to the basic flow. Unfortunately, they used an incorrect upper boundary condition in their calculations as pointed out by Olfe and Lee (1971) and Smith and Lin (1982). The heat island problem has been pursued further by some other authors (e.g., Smith 1957; Olfe and Lee 1971). This type of study has been applied to a number of different mesoscale phenomena, for example: (i) low-level heating and cooling associated with a long ridge (Raymond 1972), (ii) latent heating associated with a thunderstorm downdraft (Thorpe et al. 1980), (iii) latent heating associated with an upslope orographic rain (Smith and Lin 1982; Davies and Schar 1986), and (iv) latent heating associated with moist convection (Lin and Smith 1986; Lin 1986, 1987; Raymond 1986). Thus, this type of study appears to be helpful in improving our understanding of various mechanisms related to mesoscale dynamics.

Theoretical studies incorporating prescribed thermal forcing has also been applied to large scale flow. One of the earliest works is by Smagorinsky (1953) who has studied the steady, linear response of a large-scale flow over a prescribed, periodic heat source and sink associated with the temperature contrast of continent versus ocean. Both baroclinicity and frictional effects have been investigated by using a β-plane approximation. The linear response of large-scale flow to tropical thermal forcing has been investigated by Webster (1972), Gill (1980), Geisler (1981) and DeMaria (1985) among others. The Walker circulation, which exists to the east of tropical heat sources near the maritime continent, has been explained as the effects of the surface and elevated heating over the continent. Similar approach has also been applied to investigate the midlatitude response to tropical thermal forcing (e.g., Hoskins and Karoly 1981; Simmons 1982; Lim and Chang 1983). Those works, either use a β-plane approximation or include the β effects, are mainly for studying heat sources and sinks of planetary dimensions which produce large-scale disturbances.

For a flow over a diabatic source/sink with a horizontal scale of several hundred kilometers, the rota-

Corresponding author address: Dr. Yuh-Lang Lin, Dept. of Marine, Earth and Atmospheric Sciences, North Carolina State University, Box 8208, Raleigh, NC 27695-8208.

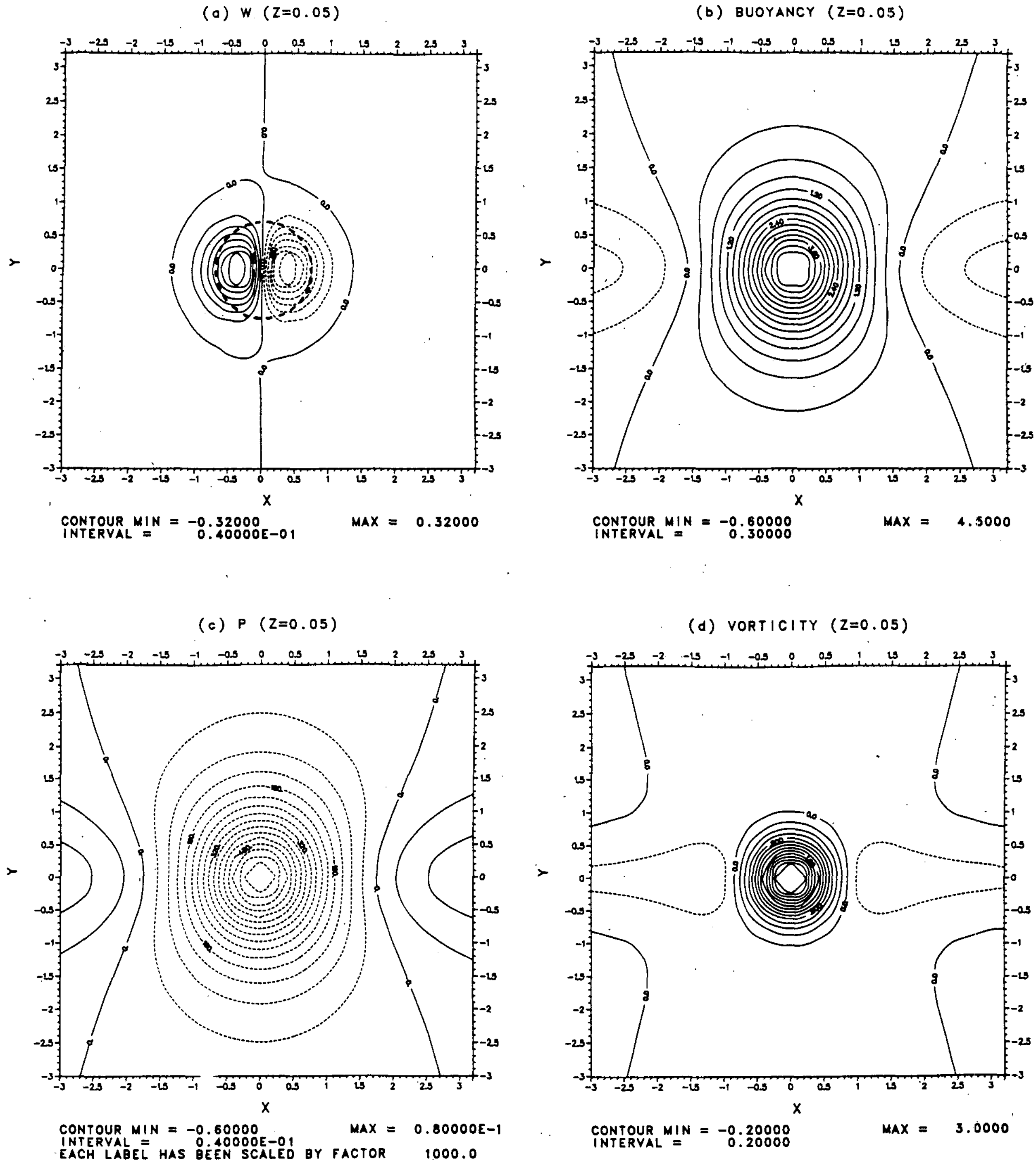

FIG. 1. Inviscid quasi-geostrophic flow over a bell-shaped warm region with the maximum perturbation potential temperature (T_0) and the half-width (a) of 7.5 and 1, respectively. The parameters associated with the basic flow are: $R_0 = 0.2$, $\gamma = 0.2$, $E = 0$. Six horizontal fields at $z = 0.05$ are shown: (a) vertical velocity, (b) buoyancy, (c) perturbation pressure, (d) relative vorticity, (e) horizontal vector wind, and (f) divergence. Three cross sections of $y = 0$ are shown: (g) vertical velocity, (h) vertical displacement, and (i) perturbation pressure. The thick dashed lines in (a) and (e) indicate the contour of $T = 4$. Notice that all variables are nondimensionalized.

tional effect plays an important role in generating inertia–gravity waves. Those waves behave differently from quasi-geostrophic planetary waves which are generated by a forcing, either thermally or orographically, with a horizontal scale of several thousand kilometers. In other words, the β-effect can be neglected,

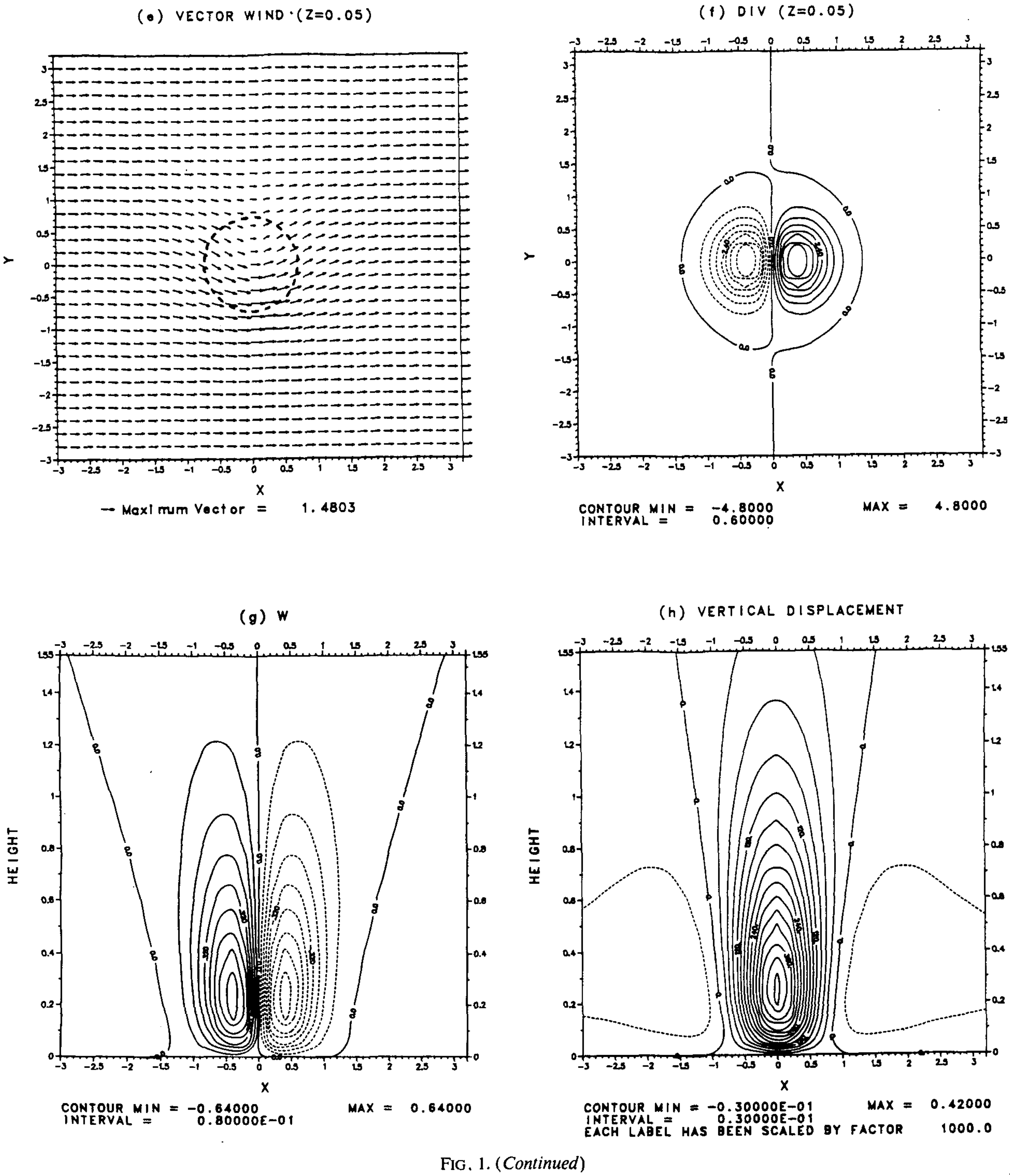

FIG. 1. (*Continued*)

but the initial effect should be included in this type of flow. Sea breezes generated by coastal differential heating and lake effects associated with diabatic heating in winter are two examples. By prescribing an isolated, diabatic heat source/sink, Rotunno (1983) has investigated the horizontal scale of the land and sea breeze circulation theoretically. Using a similar approach, Hsu (1987a) has studied the two-dimensional flow response to a prescribed, finite surface heating with thermal diffusion included. The horizontal scale of heating varies from 1 to 1000 km. This work has been extended numerically (Hsu 1987b) to include the three-dimen-

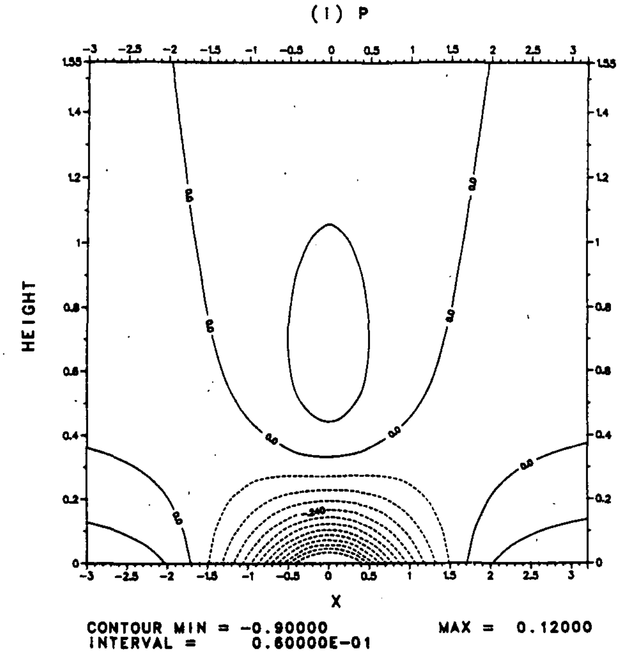

FIG. 1. (*Continued*)

sionality and apply to the snowstorm problem of Lake Michigan. Some interesting results have been obtained by Hsu by varying the shape of the diabatic heating and the basic wind directions. However, the energy propagation of the heating-induced inertia-gravity waves has not been emphasized, which need to be investigated for a better understanding of the dynamics.

A corresponding mathematical problem, which has been studied by several authors (e.g., Smith 1980), is the airflow past a three-dimensional, isolated mountain with no rotational effects included. With rotational effects included, a leftward (in the Northern Hemisphere) deflection of the air is observed as it approaches major mountain ranges such as the New Zealand Alps, Iceland and Central Mountain Range of Taiwan (Smith 1982). Based on a power series expansion in the Rossby number, Buzzi and Tibaldi (1977) have investigated the inertial and frictional effects on rotating and stratified flow over an isolated topography. They found that the disturbance associated with orographic forcing becomes asymmetric in the front–rear direction, generating a long tail of positive relative vorticity to the lee side of the mountain, with the addition of an Ekman layer in a quasi-geostrophic flow. An increase in potential vorticity is produced because the anticyclonic vorticity above the mountain tends to decay due to friction. In applying the theory to the flow over and around the Alps, their results are consistent with the observed high–low pressure pattern. However, it is not clear how the flow responds to an isolated thermal forcing under a similar situation since the airflow may behave differently, as found in some diabatic heating simulations in a nonrotating flow (e.g., Smith and Lin 1982; Lin and Smith 1986).

The problem of a stratified hydrostatic airflow past an isolated warm region will be investigated by a linear theory. Analytical solutions will be obtained in the Fourier space and transformed back to the physical space by a Fast Fourier Transform algorithm. Section 2 describes the governing equations. The response of a quasi-geostrophic inviscid flow past a bell-shaped warm region is then presented in section 3. The inertial effects and the frictional effects are investigated in sections 4 and 5. Concluding remarks are made in the last section.

2. Governing equations

The steady-state, small-amplitude equations for a stratified, hydrostatic, Boussinesq flow in a rotating system may be written

$$Uu'_{x'} - fv' = -\pi'_{x'} \quad (1)$$

$$Uv'_{x'} + fu' = -\pi'_{y'} \quad (2)$$

$$\pi'_{z'} = b' \quad (3)$$

$$u'_{x'} + v'_{y'} + w'_{z'} = 0 \quad (4)$$

$$Ub'_{x'} + N^2 w' = (g/c_p \bar{T})q' \quad (5)$$

where

- u' perturbation velocity in the x-direction
- v' perturbation velocity in the y-direction
- w' vertical velocity
- π' perturbation kinetic pressure (p'/ρ_0)
- b' perturbation buoyancy ($g\theta'/\theta_0$)
- U basic state velocity in x direction
- b_0 basic state buoyancy
- ρ_0 basic state density
- $\bar{T}$ basic state temperature
- N Brunt–Väisälä frequency ($(db_0/dz)^{1/2}$)
- f Coriolis parameter
- g gravitational acceleration
- c_p specific heat capacity at constant pressure
- q' heating rate per unit mass.

The incoming velocity (U) and the Brunt–Väisälä frequency (N) are assumed to be constant with height throughout this study. The set of Eqs. (1)–(5) can be nondimensionalized

$$\text{Ro}u_x - v + \pi_x = 0 \quad (6)$$

$$\text{Ro}v_x + u + \pi_y = 0 \quad (7)$$

$$\pi_z - b = 0 \quad (8)$$

$$u_x + v_y + \text{Ro}w_z = 0 \quad (9)$$

$$b_x + w = q \quad (10)$$

where Ro = U/fa is the Rossby number. The horizontal scale, a, is chosen to be the half-width or the scale of the heat source. The nondimensional variables are defined as following:

$$(x, y) = (x'/a, y'/a); \qquad z = z'/H_0;$$
$$(u, v) = (u'/U, v'/U); \qquad w = w'a/(\mathrm{Ro}UH_0);$$
$$\pi = \pi'/(fUa); \qquad b = b'gH_0/(fb_0Ua);$$
$$q = q'gH_0/(c_p\bar{T}U^2f). \tag{11}$$

In the above equations, a deformation depth (e.g., see Buzzi and Tibaldi 1977; Pierrehumbert and Wyman 1985), $H_0 = fa/N$, has been adopted.

Equations (6)–(10) can be reduced to a single equation of pressure by making the quasi-geostrophic approximation, i.e. retaining the zeroth and first orders of the expansion in powers of Ro (for details, see Pedlosky 1982)

$$\frac{\partial}{\partial x}(\pi_{zz} + \nabla_H{}^2\pi) = q_z. \tag{12}$$

The lower boundary condition, with Ekman friction (Charney and Eliassen 1949) included, over a flat surface requires

$$w' = -\left(\frac{U}{N^2}\right)\pi'_{xz} + \left(\frac{g}{c_p\bar{T}N^2}\right)q' = H_0\left(\frac{1}{2}E^{1/2}\right)\zeta' \quad \text{at} \quad z' = 0 \tag{13}$$

where $E = \nu/(fH_0{}^2)$ is the Ekman number and ζ' is the vertical component of the relative vorticity (Eq. (26)). The nondimensional form of (13) can be written

$$\pi_{xz} + [(E^{1/2}/2)/\mathrm{Ro}]\zeta = q \quad \text{at} \quad z = 0. \tag{14}$$

For a low-level thermal forcing we assume

$$q'(x', y', z') = h'(x', y')e^{-z'/H_1}, \tag{15}$$

where $h'(x', y')$ is the horizontal distribution of the heating and H_1 is the e-fold depth of the heating. The above equation can be expressed in nondimensional form

$$q(x, y, z) = h(x, y)e^{-z/\gamma} \tag{16}$$

where $\gamma = H_1/H_0 = NH_1/fa$ is the aspect ratio of the heating depth to the vertical scale of the flow.

To solve the problem, we make the double Fourier transform in x and y ($x \to k$, $y \to l$) of Eqs. (12), (14) and (16),

$$\hat{\pi}_{zz} - K^2\hat{\pi} = -(\hat{h}/i\gamma k)e^{-z/\gamma} \tag{17}$$

$$\hat{\pi}_z - \left(\frac{\frac{1}{2}E^{1/2}K^2}{\mathrm{Ro}ik}\right)\hat{\pi} = \frac{\hat{h}(k, l)e^{-z/\gamma}}{ik} \quad \text{at} \quad z = 0. \tag{18}$$

The relationship between pressure and vorticity, Eq. (24), has been used in deriving Eq. (18).

The general solution of Eq. (17) can be written

$$\hat{\pi} = Ae^{-Kz} + Be^{Kz} - \frac{\hat{h}\gamma e^{-z/\gamma}}{ik(1 - \gamma^2K^2)}. \tag{19}$$

The upper boundary condition requires $\pi \to 0$, which implies $B = 0$. After applying the lower boundary condition (18), the solution in the Fourier space can be obtained

$$\hat{\pi} = \frac{\hat{h}\gamma}{ik(1 - \gamma^2K^2)}\left[K\left\{\gamma + \frac{(E^{1/2}/2)(1 - \gamma K)}{\mathrm{Ro}ik + (E^{1/2}/2)K}\right\} \times e^{-Kz} - e^{-z/\gamma}\right]. \tag{20}$$

Other variables are related to π by the following relationships:

$$w = -\pi_{xz} + q, \tag{21}$$
$$u = -\pi_y, \tag{22}$$
$$v = \pi_x, \tag{23}$$
$$\zeta = \nabla_H{}^2\pi, \tag{24}$$
$$\delta = \mathrm{Ro}(\pi_{xzz} - q_z), \tag{25}$$

where

$$\zeta = v_x - u_y \quad \text{(the vertical component of the relative vorticity)} \tag{26}$$
$$\delta = u_x + v_y \quad \text{(the horizontal divergence)}. \tag{27}$$

Making Fourier transforms of Eq. (21) and using Eq. (20), the nondimensional form of the vertical velocity can be found

$$\hat{w} = \frac{\hat{h}\gamma K^2}{1 - \gamma^2K^2}\left[\left\{\gamma + \frac{(E^{1/2}/2)(1 - \gamma K)}{\mathrm{Ro}ik + (E^{1/2}/2)K}\right\}e^{-Kz} - \gamma e^{-z/\gamma}\right]. \tag{28}$$

Other variables can then be found from the Fourier transforms of Eqs. (22)–(25) and π.

For simplification, the perturbation potential temperature associated with a warm region due to low-level sensible heating is assumed to be a bell-shaped function such as

$$T'(x, y) = \frac{T'_0}{(r'^2/a^2 + 1)^{3/2}} \tag{29}$$

where $r'^2 = x'^2 + y'^2$. To the first approximation, the diabatic heating rate associated with the above specified warm region in a basic flow (U) can be specified as

$$\frac{q'}{c_p} = \frac{D\theta}{Dt} = U\frac{\partial T'}{\partial x'} + \left(\frac{N^2\theta_0}{g}\right)w'. \tag{30}$$

As discussed in Stern and Malkus (1953), the diabatic heating rate is mainly created and maintained by hor-

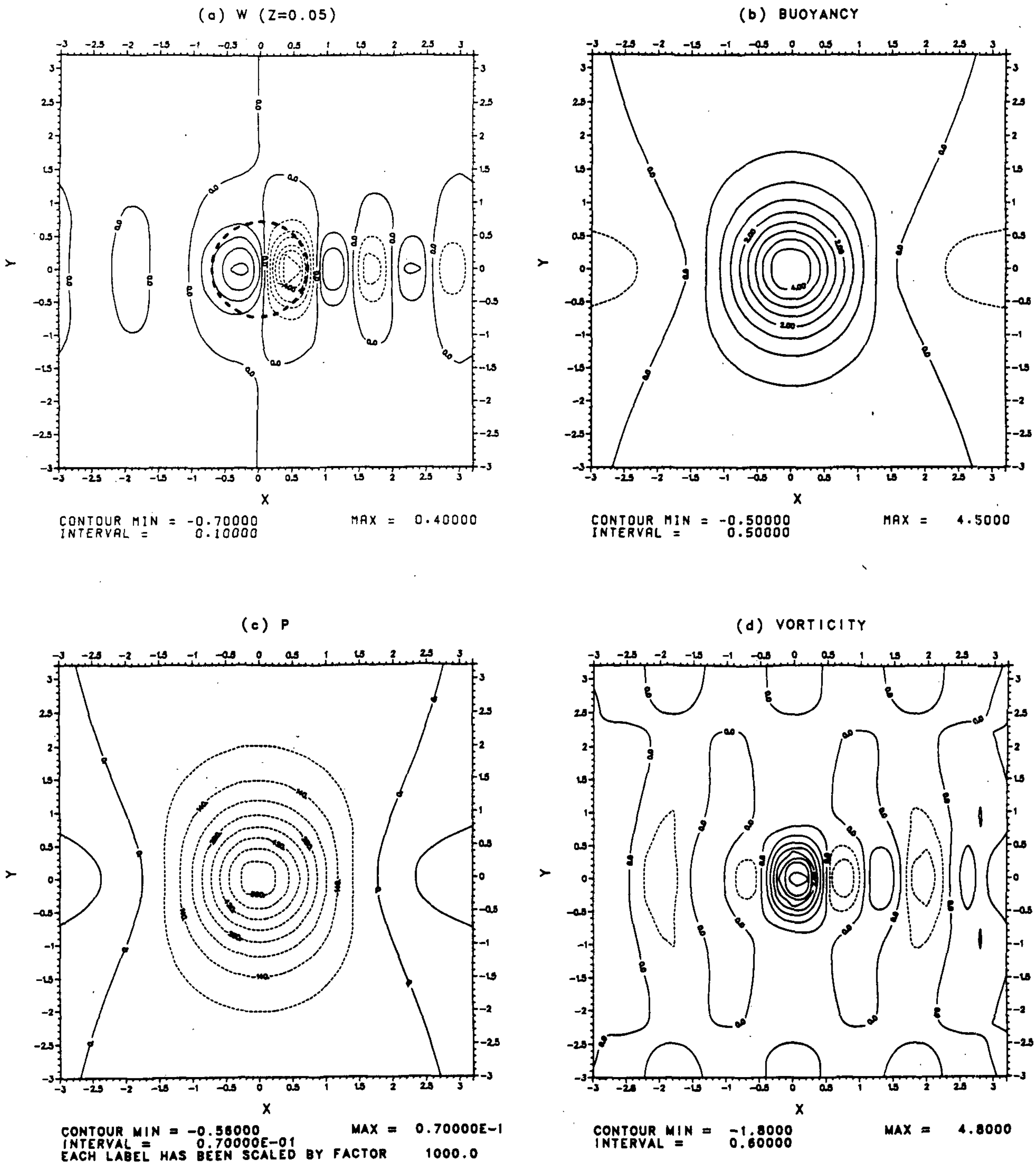

FIG. 2. As in Fig. 1 except with inertial effects included. Solutions can be found in Eqs. (36)–(45).

izontal temperature advection due to small-scale turbulence, and is not altered significantly by convective motions of the scale of w'. That is, $(N^2\theta_0/g)w' \ll U\partial T'/\partial x'$. Thus, the boundary value of q' is simply related to the horizontal temperature advection,

$$q'(x', y', 0) = h'(x', y') = c_p U \partial T'/\partial x'. \quad (31)$$

After making Fourier transforms of (29) and (31), the nondimensional form of the diabatic heating rate can be written

$$\hat{h}(k, l) = iT_0 k e^{-K}/2\pi. \quad (32)$$

Substituting Eq. (32) into Eqs. (20) and Eqs. (21)–

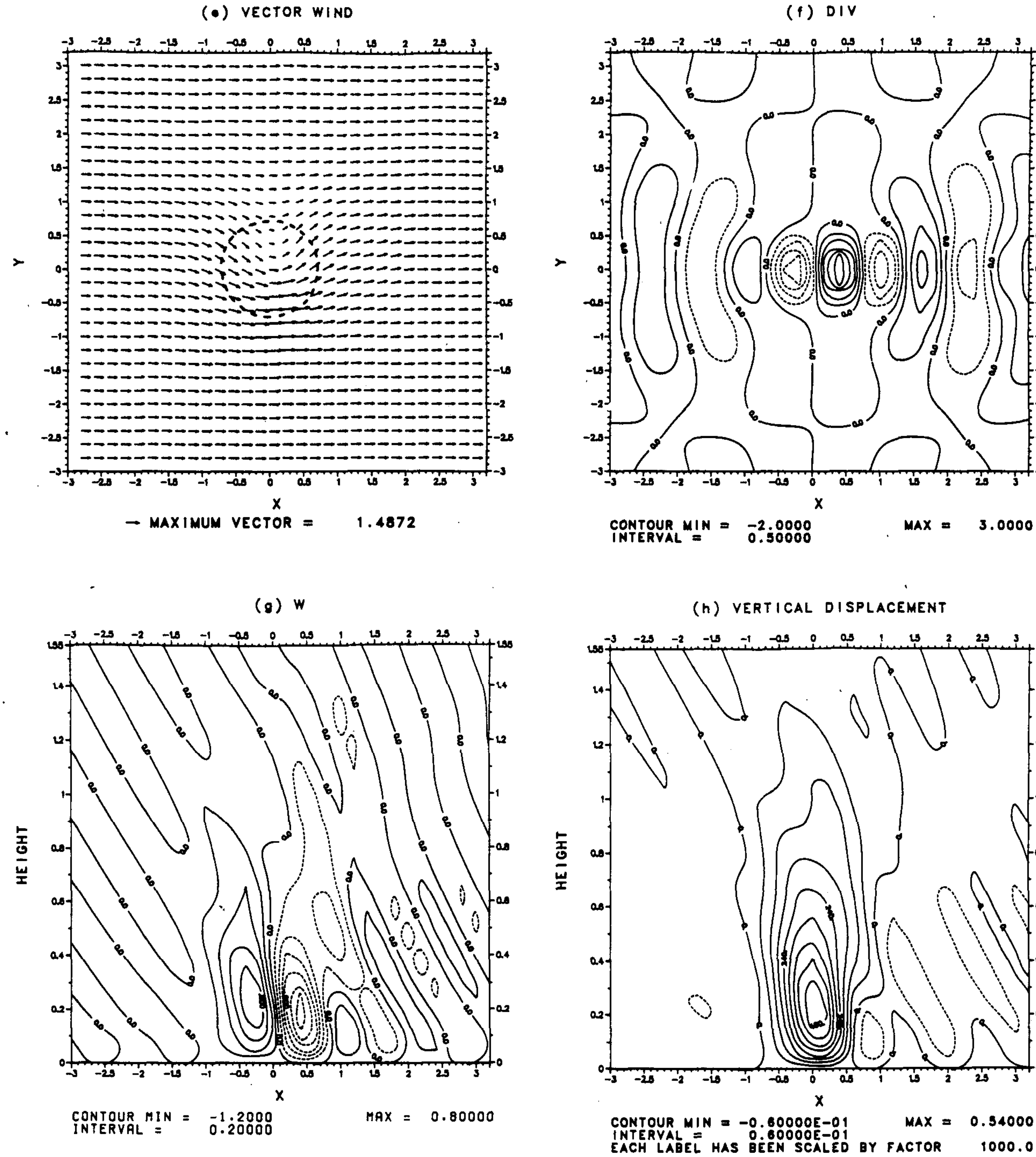

FIG. 2. (*Continued*)

(25) in Fourier space, the variables $\hat{\pi}$, $\hat{w}$, $\hat{u}$, $\hat{v}$, $\hat{\zeta}$ and $\hat{\delta}$ can be solved analytically in the Fourier space. Closed forms of the solution in the physical space are possible but tedious. Instead, the inverse Fourier transform is performed numerically by an algorithm of Fast Fourier Transform (FFT). A brief summary of the FFT scheme may be found in Smith (1980).

3. The quasi-geostrophic inviscid flow

Figure 1 shows a case of the quasi-geostrophic inviscid flow over an isolated warm region. The warm region is assumed to have a bell shape with the maximum temperature and the half-width of 7.5 and 1, respectively. The basic airflow blows from the left to

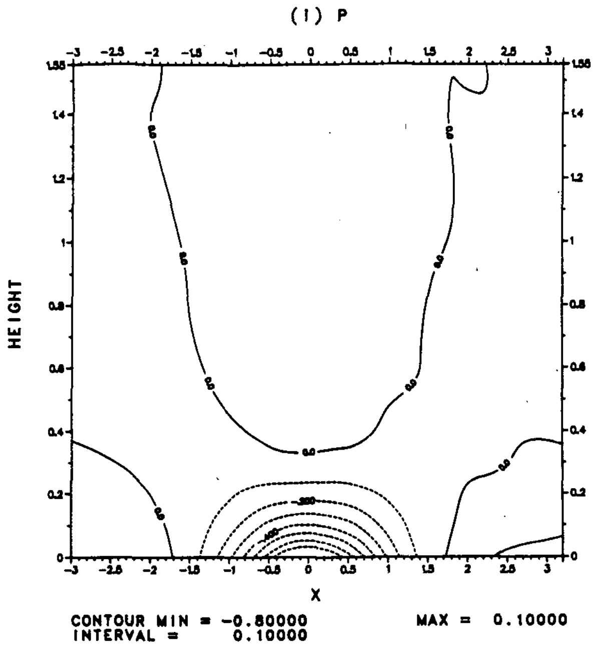

FIG. 2. (*Continued*)

the right. Therefore, there exists a heating (cooling) upstream (downstream) of the center of the warm region according to Eqs. (16) and (30). Both Ro and γ associated with the flow have a value of 0.2. The dimensional parameters may be considered as $U = 10$ m s^{-1}, $a = 500$ km, $f = 10^{-4}$ s^{-1}, $N = 0.01$ s^{-1}, $H_1 = 1$ km, $H_0 = 5$ km, and $T'_0 = 20$°C. The response of the fluid to the heating and cooling associated with the warm region at $z = 0.05$, corresponding to a dimensional height of 250 m, is an upward (downward) motion upstream (upward) of the center of the warm region (Fig. 1a). Upstream (downstream) of the region of upward (downward) motion, there exists a region of weak compensating downward (upward) motion. In fact, the vertical velocity field is in phase with the diabatic heating. The thermal forcing produces a region of high buoyancy (less dense) air in the vicinity of the warm region (Fig. 1b), which then produces the low pressure region near the surface (Fig. 1c) according to the hydrostatic balance. On both upstream and downstream sides of the region of high buoyancy and low pressure, there exist regions of weak low buoyancy and high pressure, respectively. These are associated with the weak compensative vertical displacements as displayed in Fig. 1h for a cross section along $y = 0$. At this level ($z = 0.05$), the fluid parcel experiences a cyclonic circulation near the center of the low pressure region where there exists a cell of positive relative vorticity (Fig. 1d and 1e). Two regions of weak negative vorticity appear to be on both upstream and downstream sides of the positive vorticity. Notice that the relative vorticity reaches a maximum of about $0.6f$, which is relatively high for a quasi-geostrophic approximation to be valid. Figure 1f shows the divergence field at $z = 0.05$, which has a convergence (divergence) upstream (downstream) of the center of the warm region. The divergence field is related to the vertical motion by the relationship $\delta = -w_z$.

Figure 1g–i displays the vertical cross sections of the the vertical velocity, vertical displacement and perturbation pressure along $y = 0$. Both fields show a symmetric pattern with respect to the line of $x = 0$. The vertical velocity field (Fig. 1g) near the warm region center is mainly dominated by an upward motion upstream followed by a downward motion. The absolute value of the vertical velocity increases with height until $z = 0.2$ and then decreases. Weak compensative downward and upward motions are found far upstream and downstream, respectively. The air parcel is lifted near the center of warm region and displaced downward slightly far upstream and downstream (Fig. 1h). The vertical displacement field also indicates that there exist a strong vortex stretching near the center of the warm region and two regions of weak vortex compression far upstream and downstream. The pressure disturbance (Fig. 1i) is almost confined below the *e*-fold depth of the heating, i.e. $z = 0.2$. Near the warm region center, the perturbation pressure decreases exponentially with height and reverses its phase at a level of about $z = 0.35$. The resulting region of high pressure is associated with the compensative divergence at this level, instead of convergence at lower levels. The amplitude of the perturbation pressure decays exponentially with height as also can be detected from the solution, i.e. Eq. (20).

4. Inertial effects

Equations (6)–(10) can be combined to a single equations of w,

$$\mathrm{Ro}^2 w_{xxzz} + w_{zz} + \nabla_H{}^2 w = \nabla_H{}^2 q. \tag{33}$$

Making Fourier transforms of the above equation and Eq. (16) gives

$$\hat{w}_{zz} + \frac{K^2}{\mathrm{Ro}^2 k^2 - 1}\hat{w} = \frac{\hat{h} K^2 e^{-z/\gamma}}{\mathrm{Ro}^2 k^2 - 1}. \tag{34}$$

The general solution of Eq. (34) can be written

$$\hat{w} = A e^{iKz/(\mathrm{Ro}^2k^2-1)^{1/2}} + B e^{-iKz/(\mathrm{Ro}^2k^2-1)^{1/2}} + \frac{\gamma^2 K^2 \hat{h} e^{-z/\gamma}}{\gamma^2 K^2 + (\mathrm{Ro}^2 k^2 - 1)}. \tag{35}$$

The lower boundary condition requires $w = 0$ at $z = 0$. The solution composes two parts: (a) $\mathrm{Ro}^2 k^2 > 1$ and (b) $\mathrm{Ro}^2 k^2 < 1$. For $\mathrm{Ro}^2 k^2 > 1$, the upper boundary condition requires $B = 0$ to radiate the energy upward to infinity. With the lower boundary condition applied, the solution may be written

$$\hat{w} = \frac{-\gamma^2 K^2 \hat{h}}{(\mathrm{Ro}^2 k^2 - 1) + \gamma^2 K^2}\left[e^{iKz/(\mathrm{Ro}^2k^2-1)^{1/2}} - e^{-z/\gamma}\right], \quad \text{for} \quad \mathrm{Ro}^2 k^2 > 1. \tag{36}$$

For $\mathrm{Ro}^2k^2 < 1$, the general solution can be written

$$\hat{w} = Ae^{Kz/(1-\mathrm{Ro}^2k^2)^{1/2}} + Be^{-Kz/(1-\mathrm{Ro}^2k^2)^{1/2}} + \frac{\gamma^2K^2\hat{h}e^{-z/\gamma}}{\gamma^2K^2 + (\mathrm{Ro}^2k^2 - 1)}. \quad (37)$$

The upper boundary condition requires the solution to vanish at infinity. Thus it implies that $A = 0$ and the solution reads

$$\hat{w} = \frac{\gamma^2K^2\hat{h}}{(1 - \mathrm{Ro}^2k^2) - \gamma^2K^2}[e^{-Kz/(1-\mathrm{Ro}^2k^2)^{1/2}} - e^{-z/\gamma}], \quad \text{for} \quad \mathrm{Ro}^2k^2 < 1. \quad (38)$$

The other variables can be obtained from the Fourier transforms of Eqs. (6)–(10),

$$\hat{\pi} = \frac{1}{ik}\left[\int_z^\infty \hat{w}dz - \int_z^\infty \hat{h}e^{-z/\gamma}dz\right], \quad (39)$$

$$\hat{u} = \frac{\mathrm{Ro}^2k^2 - il}{1 - \mathrm{Ro}^2k^2}\hat{\pi}, \quad (40)$$

$$\hat{v} = \frac{k(\mathrm{Ro}l + i)}{1 - \mathrm{Ro}^2k^2}\hat{\pi}, \quad (41)$$

$$\hat{b} = \frac{1}{ik}(\hat{q} - \hat{w}). \quad (42)$$

The analytic forms of π are

$$\hat{\pi} = \frac{-\hat{h}\gamma(\mathrm{Ro}^2k^2 - 1)^{1/2}}{ik[\gamma^2K^2 + (\mathrm{Ro}^2k^2 - 1)]}[i\gamma Ke^{iKz/(\mathrm{Ro}^2k^2-1)^{1/2}} + (\mathrm{Ro}^2k^2 - 1)^{1/2}e^{-z/\gamma}], \quad \mathrm{Ro}^2k^2 > 1 \quad (43a)$$

$$\hat{\pi} = \frac{\hat{h}\gamma(1 - \mathrm{Ro}^2k^2)^{1/2}}{ik[(1 - \mathrm{Ro}^2k^2) - \gamma^2K^2]}[\gamma Ke^{-Kz/(1-\mathrm{Ro}^2k^2)^{1/2}} - (1 - \mathrm{Ro}^2k^2)^{1/2}e^{-z/\gamma}], \quad \mathrm{Ro}^2k^2 < 1. \quad (43b)$$

The vorticity and divergence can be derived from the definitions (26) and (27),

$$\hat{\zeta} = -K^2\hat{\pi} - i\mathrm{Ro}^2k\hat{w}_z \quad (44)$$

$$\hat{\delta} = -\mathrm{Ro}\hat{w}_z. \quad (45)$$

Notice that the second order of the expansion in powers of Ro enters in the formula of the relative vorticity.

Figure 2 shows a case similar to that of Fig. 1 except with the inertial terms included. Compared with the quasi-geostrophic case, the vertical motion near the diabatic source is strengthened and there exists dispersed disturbances downstream (Fig. 2a and 2g). The maximum amplitude of the downward vertical velocity is more than double value of the quasi-geostrophic case. This is mainly caused by the advection effect. The vertical cross section along $y = 0$ (Fig. 2g) indicates that the vertical extent of the vertical motion is much smaller than that of the quasi-geostrophic case. This can be explained by the smaller e-folding depth of the vertical motion, $(1 - \mathrm{Ro}^2k^2)^{1/2}/K$ from Eq. (38), compared with that of the quasi-geostrophic case, $1/K$ from Eq. (28). The buoyancy and pressure fields (Fig. 2b, c and i) are very similar to that of the quasi-geostrophic case with only slight differences in amplitudes. The vorticity field is much stronger than the previous case, with a maximum increased by a factor of 1.5 and a more compact horizontal extent. By comparing Eq. (44) and the Fourier transform of Eq. (24), the difference of the vorticity fields is caused by the inertial effects, i.e. the second term of Eq. (44). The vertical gradient of the vertical velocity is large for the present case because of the smaller vertical extent of the vertical motion as mentioned earlier. This tends to strengthen the vorticity field. Associated with the stronger vorticity near the diabatic source region, the horizontal wind field shows a stronger cyclonic circulation. The compact and wavy structure, similar to the vertical velocity field, also appears in the vorticity, divergence, and vertical displacement fields. The upstream phase tilt of the vertical velocity and displacement fields indicates an upward propagation of the inertia–gravity waves, even though it is weak for such a small Rossby number flow.

Figure 3 shows a case of an inviscid flow with Ro = 1 past an isolated warm region. The parameters associated with the flow and the diabatic source/sink are $\gamma = 1.0$ and $T_0 = 1.5$. The dimensional parameters may be considered as $U = 10$ m s^{-1}, $a = 100$ km, $f = 10^{-4}$ s^{-1}, $N = 0.01$ s^{-1}, $H_0 = 1$ km, $H_1 = 1$ km, $T_0' = 4$°C. The response of the fluid to diabatic heating at $z = 0.25$, corresponding to $z' = 250$ m, is an upward motion upstream and near the center of the warm region followed by a downward motion downstream (Fig. 3a). Compared with the quasi-geostrophic case, the major regions of upward and downward motion are shifted downstream. This can be explained by the advection effect because the inertial terms, i.e. the Ro terms, of Eqs. (6)–(7) cannot be neglected in the present case. Even though not shown in Fig. 3a, there still exists a weak compensative downward motion associated with the major region of upward motion (Fig. 3g). The horizontal pattern of the vertical velocity is more asymmetric in the basic wind direction than that in the quasi-geostrophic case. The buoyancy field (Fig. 3b) is similar to that of the quasi-geostrophic case, except there exists a region of high buoyancy (less dense) air far downstream. The major region of high buoyancy near the center of the warm region is mainly produced by the diabatic heating and cooling. The indirect effect on the buoyancy due to vertical motion [Eq. (10)] is not pronounced at such a low level because the vertical velocity is weak near the surface.

The perturbation pressure pattern (Fig. 3c) is no longer similar to the perturbation buoyancy pattern as that of quasi-geostrophic case. This is mainly caused

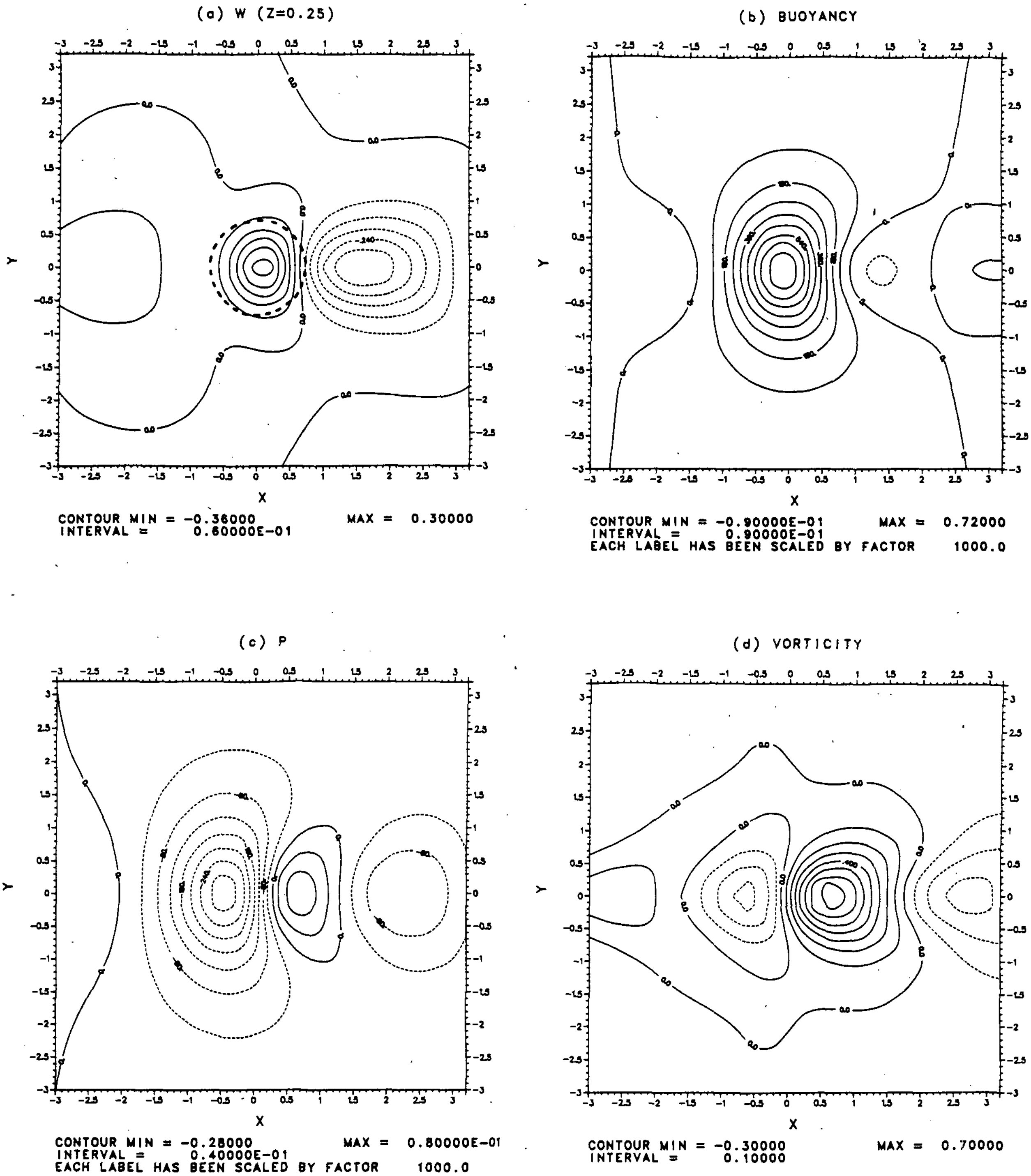

FIG. 3. As in Fig. 2 except with a larger Rossby number. The parameters used are: $T_0 = 1.5$, $a = 1$, Ro = 1, and $\gamma = 1$. The horizontal fields plotted are at $z = 0.25$. The thick dashed lines in (a) and (e) indicate the contour of $T = 0.8$.

by the vertical propagation of the thermally induced inertia-gravity waves. In fact, the pressure field is almost out of phase with the buoyancy field. The U-shaped pattern of the perturbation pressure, also pronounced in other fields, is an indication of the upward propagation of energy as shown in a nonrotational mountain wave problem (Smith 1980) and in a nonrotational diabatic heating problem (Lin 1986). The

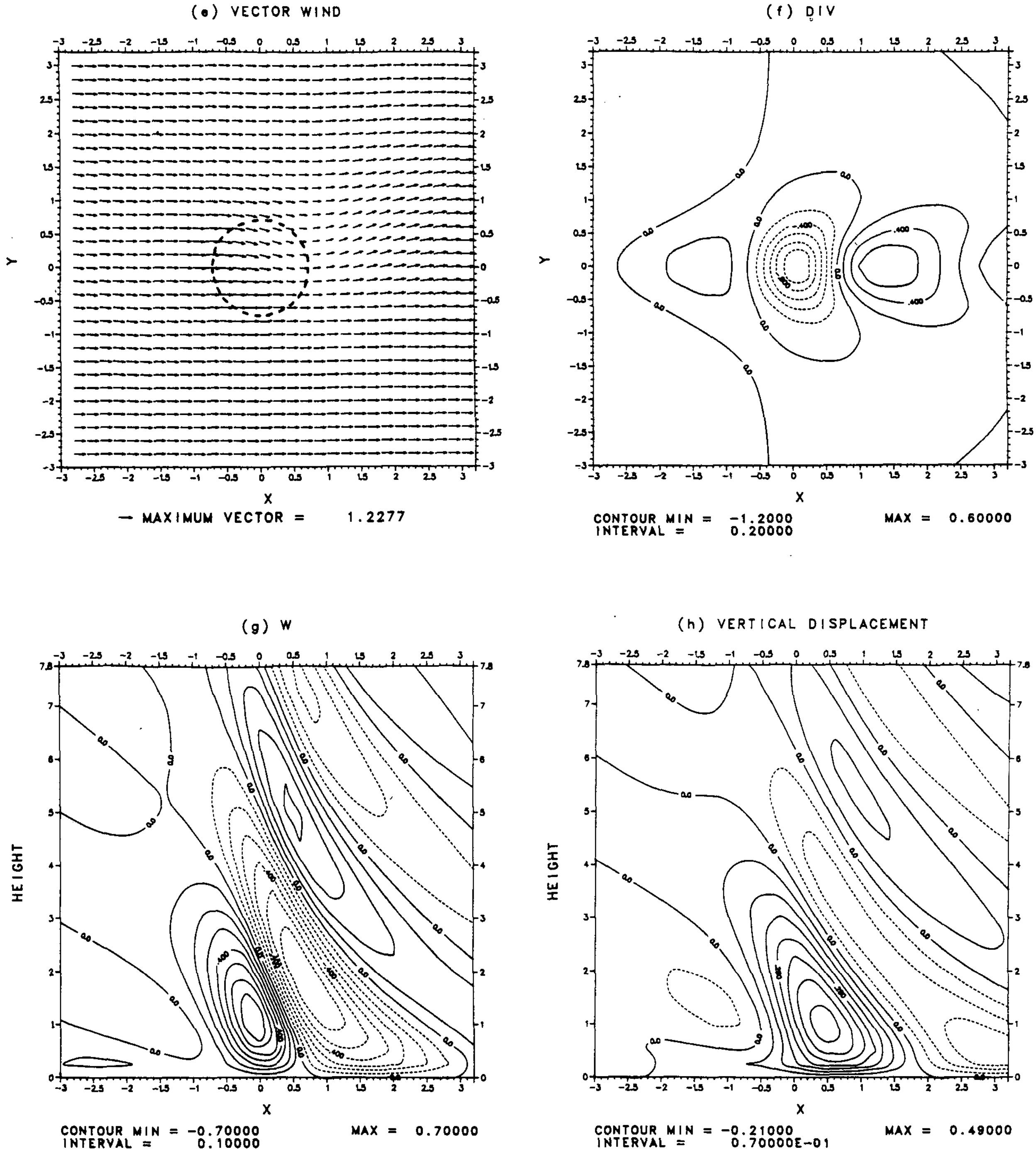

FIG. 3. (*Continued*)

group velocity calculation of Smith can be extended to include the Coriolis force (see Appendix), which gives the concentrated region of the wave energy

$$y^2 = \left[\frac{zl^2(\mathrm{Ro}^2k^2 - 1)^{1/2}}{k(\mathrm{Ro}^2l^2 - 1)(k^2 + l^2)^{1/2}}\right]x,$$

$$\mathrm{Ro}^2k^2 \geqslant 1. \qquad (46)$$

With no rotation, the above equation reduces to the formula derived by Smith. With rotational effects included, the wave energy is still concentrated near the parabola described by Eq. (46). However, the latus rectum becomes larger compared to the nonrotational case. Also, Eq. (46) indicates that only the wave part of the disturbance contributes to the upward propa-

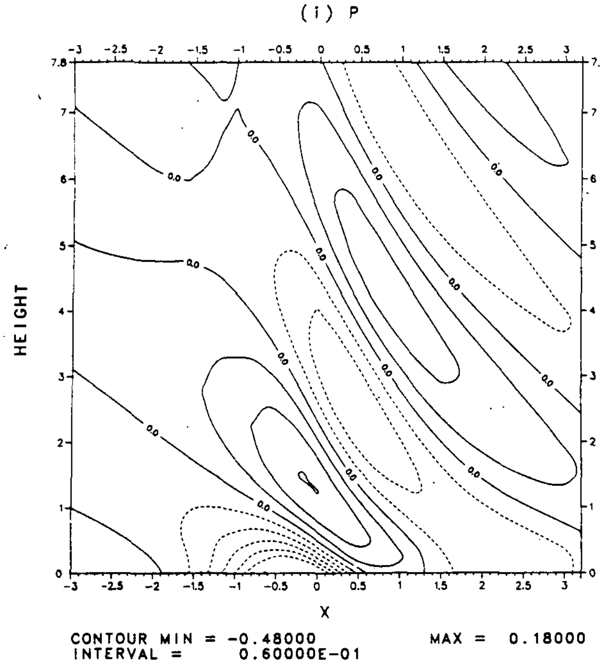

FIG. 3. (*Continued*)

gation of the energy. Therefore the U-shape is less pronounced for a flow with smaller Rossby number. Another evidence of upward propagation of wave energy is the upstream phase tilt as shown in the cross section of $y = 0$ (Fig. 3i). The regions of maximum and minimum perturbation pressures are shifted farther downstream with height, which indicates that the wave energy is propagated upward and advected downstream. There is a negative vorticity center just upstream of the center of the warm region followed by a strong positive vorticity center just downstream and a negative vorticity center far downstream (Fig. 3d). The significant difference from the quasi-geostrophic case is that the positive (negative) vorticity is associated with the high (low) pressure, and not the low (high) pressure. The positive vorticity field is no longer in phase with the low pressure because the vertical velocity term is as important as the pressure term in Eq. (44) for a flow with a larger Rossby number. Due to weaker rotational effect, the vector wind does not deflect as strongly as for the quasi-geostrophic case. However, the cyclonic flow around the region of positive vorticity, not the low pressure, is still evident in this case (Fig. 3e). The divergence field is related to the vertical velocity field by Eq. (45) (Fig. 3f). A region of convergence near the center of the warm region is accompanied by two regions of divergence upstream and downstream. Figure 3g–i shows the cross sections of the vertical velocity, vertical displacement, and pressure along $y = 0$. The major difference from the quasi-geostrophic case is that the phase tilts upstream with height. The perturbation pressure field is roughly in phase with the vertical velocity, which indicates that the wave energy is propagated upward because the vertical energy flux, $\int p'w'dx$, is positive (Eliassen and Palm 1960; Jones 1967).

5. Frictional effects

To investigate the frictional effects of a quasi-geostrophic flow past an isolated warm region, a case similar to that of Fig. 1 with the addition of an Ekman layer is investigated. The lower boundary condition (13) is applied at $z = 0$ instead of at the top of the Ekman layer. This can be considered as a linear approach by assuming the Ekman layer is very shallow. The Ekman number is assumed to be 0.01, while other parameters are kept same as that of Fig. 1. Compared with the inviscid case, the upward motion is significantly strengthened, while the downward motion is only slightly strengthened (Fig. 4a). The regions of upward and downward motion are displaced further downstream compared with the inviscid case. This downstream displacement is associated with the upstream phase tilt occurs in the lower layer as shown in the cross section (Fig. 4g). Another significant difference is the upstream–downstream asymmetry, which also occurs in other fields at $z = 0.05$.

The low-level upstream phase tilt is consistent with that of Smagorinsky (1953) who investigated a diabatic heating problem with β effects and baroclinicity included, and the upstream–downstream asymmetry is similar to that of Buzzi and Tibaldi (1977) for a mountain wave problem. These two phenomena are related by the following argument. At $z = 0$, the maximum positive vorticity is located right at the center of the warm region as can be seen from the inviscid case (Fig. 1d). According to the lower boundary condition (13) associated with the Ekman friction, the maximum upward motion will be shifted from the upstream in the interior fluid to the center of the warm region at the top of the Ekman layer ($z = 0$). Thus there exists an upstream phase tilt with height in the lower layer. The disturbance associated with the upward motion is then advected by the basic wind, which gives the asymmetric pattern of the vertical velocity. This upstream-downstream asymmetry also appears in the other fields such as the buoyancy, pressure, vorticity, and divergence (Fig. 4b–f) and can be explained in the same way. The low-level upstream phase tilt also appears in the cross sections of other fields such as the vertical displacement and pressure (Fig. 4h and 4i). Both the pressure and vorticity fields are weakened in the presence of Ekman friction. This can be explained by the "spindown" process (e.g., see Pedlosky 1982). That is, the fluid sucked out by the cyclonic vortex from the Ekman layer must flow out in the inviscid layer, from the vortex center to its rim. This outward mass flux will produce vortex compression and reduce the inward pressure-gradient force.

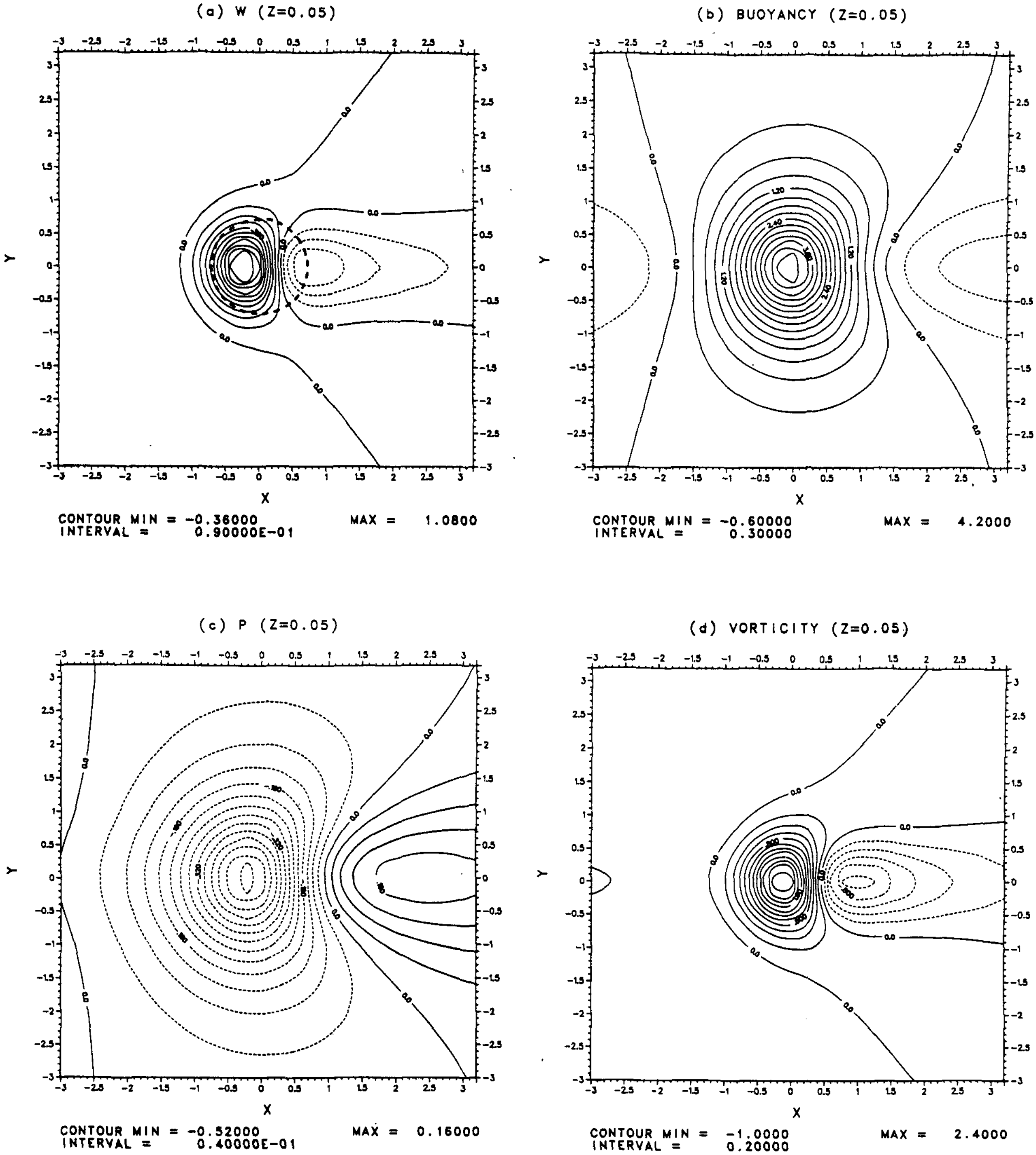

FIG. 4. As in Fig. 1 except with an Ekman layer included. The Ekman number is 0.01.

6. Concluding remarks

Inertial and frictional effects on stratified hydrostatic airflow past an isolated warm region are investigated by linear theories. For an inviscid quasi-geostrophic flow, there exists a couplet of regions of upward and downward motion in the vicinity of the warm region in the lower layer. The vertical velocity field is in phase with the diabatic heating and cooling. As expected, regions of high buoyancy, low pressure and positive vorticity are produced in the vicinity of the warm region. The wind is deflected cyclonically near the center of

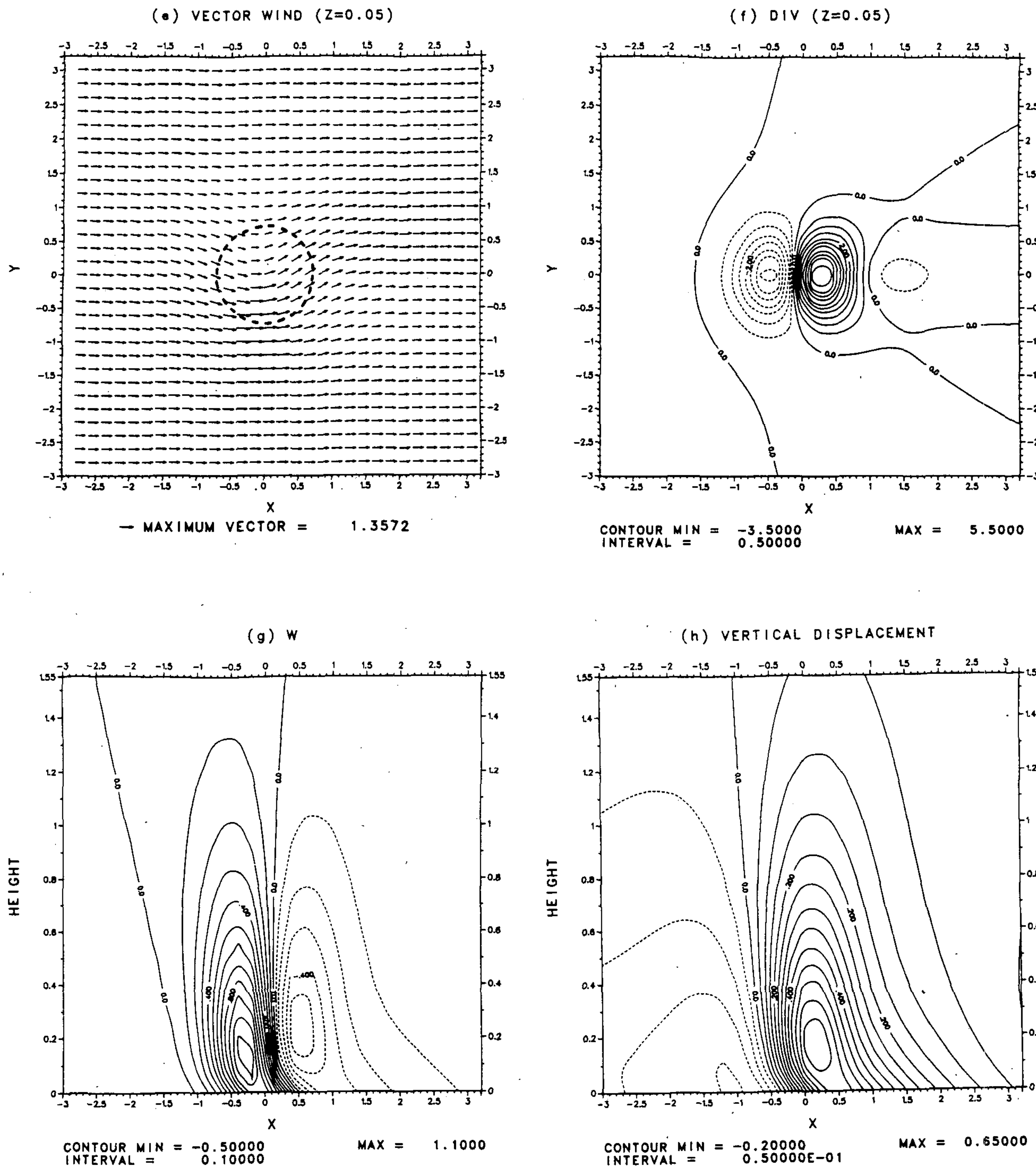

FIG. 4. (*Continued*)

the warm region. A couplet of divergence and convergence are associated with the upward and downward motions, respectively. The vertical displacement field indicates that strong vortex stretching exists near the center of the warm region, accompanied by two regions of weak vortex compression upstream and downstream. The perturbation pressure reverses its sign at higher levels, but decays exponentially with height.

With the inertial effects included, the vertical motion and the vorticity are strengthened. The horizontal wind experiences a much stronger cyclonic circulation near the diabatic source. For a flow with a larger Rossby

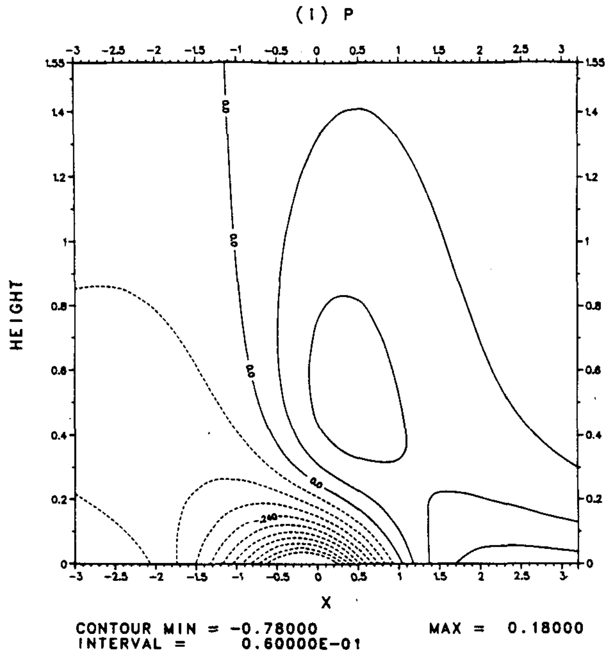

FIG. 4. (*Continued*)

number $O(1)$ over an isolated warm region, the response of the fluid to the thermal forcing is significantly different from the inviscid quasi-geostrophic case. The advection effect of the basic flow is dominant. U-shaped pattern of the disturbance are pronounced. These patterns are associated with the upward propagating inertia-gravity waves. The wind is deflected cyclonically around the region of positive relative vorticity which is advected downstream of the center of the warm region, rather than around the region of low pressure.

The frictional effects are investigated by the addition of an Ekman friction layer to a quasi-geostrophic flow. There are three significant features of the resulting disturbance: (i) an upstream–downstream asymmetry, (ii) an upstream phase tilt in the lower layer, and (iii) weakening of the positive relative vorticity and the low pressure. Items (i) and (ii) are explained by the upward motion and vorticity and the advection of the basic flow on the disturbance induced by the Ekman friction. The weakening of the positive relative vorticity and the low pressure can be explained as the spindown process of the interior flow resulting from the Ekman friction.

In this study, we have only considered prescribed heating, uniform basic wind and linear response. The theory can be extended to have a more realistic parameterization of the boundary layer physics, which will allow the feedback from the motion field to the heating. To apply the theory to the midlatitude, one should include the baroclinic effect which is treated in a separate paper. To include the nonlinear response in the inertia-gravity wave regime, one might want to consider a fully numerical modeling.

Acknowledgments. The author wishes to express his gratitude to Drs. G. S. Janowitz and A. J. Riordan of North Carolina State University for their valuable comments on this work and the review of the manuscript. This work was partially supported by the FRPD Fund of the N.C. State University under Grant 01044. Acknowledgment is made to C.-Y. Huang for helping to plot the figures.

APPENDIX

Derivation of Eq. (46)

The dispersion relation for inertia-gravity waves in a stagnant Boussinesq fluid is

$$\varpi = \pm\left[\frac{N^2(k^2+l^2)+f^2m^2}{k^2+l^2+m^2}\right]^{1/2}. \qquad \text{(A1)}$$

With hydrostatic approximation,

$$\varpi = \pm\left[\frac{N^2(k^2+l^2)+f^2m^2}{m^2}\right]^{1/2}$$

$$= \pm\frac{[N^2(k^2+l^2)+f^2m^2]^{1/2}}{m}. \qquad \text{(A2)}$$

The group velocity can be found,

$$c_{gx} = -\frac{\partial\varpi}{\partial k} = \frac{-N^2k}{m[N^2(k^2+l^2)+f^2m^2]^{1/2}}, \qquad \text{(A3)}$$

$$c_{gy} = -\frac{\partial\varpi}{\partial l} = \frac{-N^2l}{m[N^2(k^2+l^2)+f^2m^2]^{1/2}}, \qquad \text{(A4)}$$

$$c_{gz} = -\frac{\partial\varpi}{\partial m} = \frac{N^2(k^2+l^2)}{m^2[N^2(k^2+l^2)+f^2m^2]^{1/2}}. \qquad \text{(A5)}$$

For steady waves on a mean flow we replace ϖ with the intrinsic frequency Uk, so (A2) becomes

$$m = \pm\frac{N(k^2+l^2)^{1/2}}{(U^2k^2-f^2)^{1/2}}. \qquad \text{(A6)}$$

The components of the group velocity in fixed coordinates can be obtained by adding U to (A3) and using (A6)

$$c_{gx} = \frac{U^2l^2-f^2}{U(k^2+l^2)}, \qquad \text{(A7)}$$

$$c_{gy} = \frac{-l(U^2k^2-f^2)}{U(k^2+l^2)}, \qquad \text{(A8)}$$

$$c_{gz} = \frac{(U^2k^2-f^2)^{3/2}}{UNk(k^2+l^2)^{1/2}}. \qquad \text{(A9)}$$

In a reference frame fixed with earth, wave energy propagates from the energy source along straight lines with slopes

$$\frac{x}{z} = \frac{c_{gx}}{c_{gz}} \qquad \text{(A10)}$$

$$\frac{y}{z} = \frac{c_{gy}}{c_{gz}} \tag{A11}$$

$$\frac{y}{x} = \frac{c_{gy}}{c_{gx}} \tag{A12}$$

With Eqs. (A7) and (A8), we obtain

$$\frac{y}{x} = -\frac{l(U^2k^2 - f^2)}{k(U^2l^2 - f^2)}. \tag{A13}$$

Using Eqs. (A13) and (A10) lead to Eq. (46).

REFERENCES

Buzzi, A., and S. Tibaldi, 1977: Inertial and frictional effects on rotating and stratified flow over topography. *Quart. J. Roy. Meteor. Soc.*, **103**, 135–150.

Davies, H. C., and C. Schar, 1986: Diabatic modification of airflow over a mesoscale orographic ridge: A model study of the coupled response. *Quart. J. Roy. Meteor. Soc.*, **112**, 711–730.

DeMaria, M., 1985: Linear response of a stratified tropical atmosphere to convective forcing. *J. Atmos. Sci.* **42**, 1944–1959.

Eliassen, A., and E. Palm, 1960: On the transfer of energy in stationary mountain waves. *Geofys. Publ.* **22**, 1–23.

Geisler, J. E., 1981: A linear model of the Walker circulation. *J. Atmos. Sci.*, **38**, 1390–1400.

——, and F. P. Bretherton, 1969: The sea-breeze forerunner. *J. Atmos. Sci.*, **26**, 82–95.

Gill, A. E., 1980: Some simple solutions for heat-induced tropical circulation. *Quart. J. Roy. Meteor. Soc.*, **106**, 447–462.

Hoskins, B. J., and D. J. Karoly, 1981: The steady linear response of a spherical atmosphere to thermal and orographic forcing. *J. Atmos. Sci.*, **38**, 1179–1196.

Hsu, H., 1987a: A linear study of steady atmospheric flow above a finite surface heating. *J. Atmos. Sci.*, **44**, 186–199.

——, 1987b: Mesoscale lake-effect snowstorms in the vicinity of Lake Michigan: Linear theory and numerical simulations. *J. Atmos. Sci.*, **44**, 1019–1040.

Jones, W. L., 1967: Propagation of internal gravity waves in fluids with shear flow and rotation. *J. Fluid Mech.*, **30**, 439–448.

Lim, H., and C. P. Chang, 1981: A theory for midlatitude forcing of tropical motions during winter monsoons. *J. Atmos. Sci.*, **38**, 2377–2392.

Lin, Y.-L., 1986: Calculation of airflow over an isolated heat source with application to the dynamics of V-shaped clouds. *J. Atmos. Sci.*, **43**, 2736–2751.

——, 1987: Two-dimensional response of a stably statified shear flow to diabatic heating. *J. Atmos. Sci.*, **44**, 1375–1393.

——, and R. B. Smith, 1986: Transient dynamics of airflow near a local heat source. *J. Atmos. Sci.*, **43**, 40–49.

Malkus, J. S., and M. E. Stern, 1953: The flow of a stable atmosphere over a heat island. Part I. *J. Meteor.*, **10**, 30–41.

Olfe, D. B., and R. L. Lee, 1971: Linearized calculation of urban heat island convection effects. *J. Atmos. Sci.*, **28**, 1374–1388.

Pedlosky, J., 1982: *Geophysical Fluid Dynamics*. Springer-Verlag, 2nd ed., 624 pp.

Pierrehumbert, R. T., and B. Wyman, 1985: Upstream effects of mesoscale mountains. *J. Atmos. Sci.*, **42**, 977–1003.

Raymond, D. J., 1972: Calculation of airflow over an arbitrary ridge including diabatic heating and cooling. *J. Atmos. Sci.*, **29**, 837–843.

——, 1986: Prescribed heating of a stratified atmosphere as a model of moist convection. *J. Atmos. Sci.*, **43**, 1101–1111.

Rotunno, R., 1983: On the linear theory of the land and sea breeze. *J. Atmos. Sci.*, **40**, 1999–2009.

Simmons, A. J., 1982: The forcing of stationary wave motion by tropical diabatic heating. *Quart. J. Roy. Meteor. Soc.*, **108**, 503–534.

Smagorinsky, J., 1953: The dynamical influence of large-scale heat sources and sinks on the quasi-stationary mean motions of the atmosphere. *Quart. J. Roy. Meteor. Soc.*, **79**, 342–366.

Smith, R. B., 1980: Linear theory of stratified hydrostatic flow past an isolated mountain. *Tellus*, **32**, 348–364.

——, 1982: Synoptic observations and theory of orographically disturbed wind and pressure. *J. Atmos. Sci.*, **39**, 60–70.

——, 1986: Further development of a theory of lee cyclogenesis. *J. Atmos. Sci.*, **43**, 1582–1602.

——, and Y.-L. Lin, 1982: The addition of heat to a stratified airstream with application to the dynamics of orographic rain. *Quart. J. Roy. Meteor. Soc.*, **108**, 353–378.

Smith, R. C., 1957: Air motion over a heated land mass, II. *Quart. J. Roy. Meteor. Soc.*, **83**, 248–256.

Stern, M. E., and J. S. Malkus, 1953: The flow of a stable atmosphere over a heat island. Part II. *J. Meteor.*, **10**, 105–120.

Thorpe, A. J., M. J. Miller and M. W. Moncrieff, 1980: Dynamical models of two-dimensional downdraughts. *Quart. J. Roy. Meteor. Soc.*, **106**, 463–484.

Webster, P. J., 1972: Response of the tropical atmosphere to local steady forcing. *Mon. Wea. Rev.*, **100**, 518–541.